Published October 7, 2010 as 10.3174/ajnr.A2243

ORIGINAL RESEARCH

Abnormal Microstructure of the Atrophic Thalamus in Preterm Survivors with Periventricular Leukomalacia

A.C. Nagasunder
H.C. Kinney
S. Blüml
C.J. Tavaré
T. Rosser
F.H. Gilles
M.D. Nelson
A. Panigrahy

BACKGROUND AND PURPOSE: The neuroanatomic substrate of cognitive deficits in long-term survivors of prematurity with PVL is poorly understood. The thalamus is critically involved in cognition via extensive interconnections with the cerebral cortex. We hypothesized that the thalamus is atrophic (reduced in volume) in childhood survivors of prematurity with neuroimaging evidence of PVL and that the atrophy is associated with selective microstructural abnormalities within its subdivisions.

MATERIALS AND METHODS: We performed quantitative volumetric and DTI measurements of the thalamus in 17 children with neuroimaging evidence of PVL (mean postconceptional age, 5.6 ± 4.0 years) who were born prematurely and compared these with 74 term control children (5.7 ± 3.4 years).

RESULTS: The major findings were the following: 1) a significant reduction in the overall volume of the thalamus in patients with PVL compared with controls ($P < .0001$), which also correlated with the severity of PVL ($P = .001$); 2) significantly decreased FA ($P = .003$) and increased $\lambda_\perp$ ($P = .02$) in the thalamus overall and increased axial, radial, and mean diffusivities in the pulvinar ($P < .03$), suggesting injury to afferent and efferent myelinated axons; and 3) a positive correlation of pulvinar abnormalities with those of the parieto-occipital white matter in periventricular leukomalacia, suggesting that the pulvinar abnormalities reflect secondary effects of damaged interconnections between the pulvinar and parieto-occipital cortices in the cognitive visual network.

CONCLUSIONS: There are volumetric and microstructural abnormalities of the thalamus in preterm children with PVL, very likely reflecting neuronal loss and myelinated axonal injury. The selective microstructural damage in the pulvinar very likely contributes to abnormal cognitive visual processing known to occur in such survivors.

ABBREVIATIONS: A= anterior, ADC or D_{av} = apparent diffusion coefficient or mean diffusivity; ANOVA = analysis of variance; CVI = cognitive visual impairment; DTI = diffusion tensor imaging; FA = fractional anisotropy; FLAIR = fluid attenuated inversion recovery; L = lateral; $\lambda_\parallel$ = axial diffusivity; λ_1 = eigenvalue 1; λ_2 = eigenvalue 2; λ_3 = eigenvalue 3; $\lambda_\perp$ = radial diffusivity; M = medial dorsal; P = pulvinar; PCA = postconceptional age; PVL = periventricular leukomalacia; *R* = Pearson correlation; RA = relative anisotropy; VR = volume ratio

PEDIATRICS

ORIGINAL RESEARCH

Preterm infants are highly vulnerable to brain injury resulting in a substantial burden of cognitive disability,[1] but the neuroanatomic substrate of the cognitive impairments is not completely understood.[1,2] A major neuropathologic finding in preterm infants is PVL, a disorder of immature cerebral white matter characterized by focal periventricular necrosis and diffuse gliosis in the surrounding white matter.[2,3] Emerging neuropathologic and neuroimaging studies indicate that PVL does not occur in isolation but rather is associated with injury to gray matter sites, including the thalamus, cerebral cortex, hippocampus, basal ganglia, cerebellum, and brain stem in variable combinations.[1,2] This spectrum of gray and white matter injuries is now referred to as the "encephalopathy of prematurity."[1,2] Indeed, the associated damage to certain gray matter regions that are critical to higher cognitive processing may account for the intellectual deficits in preterm survivors with PVL. Of the gray matter structures involved in the encephalopathy of prematurity, the thalamus is critically involved in cognition via extensive interconnections with the cerebral cortex.

A recent neuropathologic study of the thalamus in PVL indicates that damage to this structure is present in most (59%) postmortem examinations.[4] The incidence of such injury in published neuroimaging studies in living children is lower,[5-10] very likely reflecting variability in living versus postmortem cohorts and/or incomplete sensitivity of the neuroimaging techniques to detect subtle neuronal loss and/or gliosis observed in histologic sections. MR imaging studies indicate a diminished volume of the thalamus in PVL,[11-13] consistent with atrophy due to diffuse neuronal loss and gliosis

Received May 18, 2010; accepted after revision June 9.

From the Department of Radiology (A.C.N., S.B., M.D.N., A.P.), Division of Neuropathology, Department of Pathology (C.J.T., F.H.G.), and Division of Neurology (T.R.), Department of Pediatrics, Childrens Hospital, Los Angeles, California; Department of Biomedical Engineering (A.C.N.), University of Southern California, Los Angeles, California; Department of Pathology (H.C.K.), Children's Hospital Boston, Harvard Medical School, Boston, Massachusetts; Rudi Schulte Research Institute (S.B.), Santa Barbara, California; and Department of Pediatric Radiology (A.P.), Children's Hospital of Pittsburgh of UPMC, Pittsburgh, Pennsylvania.

This work was supported by the Rudi Schulte Research Institute; National Institutes of Health (NS063371); and Childrens Hospital Los Angeles General Clinical Research Center (CCI-06–00121).

Please address correspondence to Ashok Panigrahy, MD, Department of Pediatric Radiology, Children's Hospital of Pittsburgh of UPMC, 45th St and Penn Ave, Pittsburgh, PA 15201; e-mail: panigrahya@upmc.edu

DOI 10.3174/ajnr.A2243

detected by neuropathologic examination.[4,14] Most important, decreased thalamic volume in association with PVL correlates with cognitive deficits in survivors.[10,12,13]

In the following study, we applied the technique of DTI to obtain much-needed information about intrinsic thalamic microstructural pathology in childhood survivors of prematurity with PVL. DTI is a noninvasive advanced imaging technique that enables the measurement of the random motion of water molecules to provide information regarding "microstructure," (ie, cellular and subcellular integrity and pathology of the tissue).[15,16] It measures the following: 1) anisotropy, an index of the directional diffusivity of water in relation to the magnitude and orientation of structure; and 2) diffusivity, an index of the rate of water diffusion with preference to a specific direction. In myelinated tissue, $\lambda_\perp$ correlates with demyelination, while $\lambda_\parallel$ correlates with axonal injury, as determined by correlations between neuroimaging and histopathology in animal models.[17-19] DTI has been used to study corticothalamic connections in survivors of prematurity,[20-22] but these studies rely only on tractography postprocessing methods based on FA. In contrast, our study measures diffusivity DTI metrics within the thalamic parenchyma, thereby providing information about its intrinsic cellular pathology. In our study, we tested the hypothesis that the thalamus is atrophic (reduced in volume) in childhood survivors of prematurity with PVL (diagnosed by conventional MR imaging) and that the atrophy is associated with microstructural abnormalities within its subdivisions. We sought to determine, in particular, whether there is targeted involvement of microstructural abnormalities in the posterior subdivision of the thalamus (pulvinar) as a potential reflection of the preferential involvement of the posterior (parieto-occipital) white matter in PVL.

Materials and Methods

Subjects

The inclusion criteria for the preterm survivors with PVL were the following: 1) prematurity (<37 gestational weeks at birth), and 2) evidence of the sequelae of PVL on conventional MR imaging performed during childhood. These sequelae were defined as periventricular white matter volume loss and signal-intensity hyperintensities on FLAIR.[23] PVL was classified as mild, moderate, or severe on the basis of the degree of posterior lateral ventriculomegaly and the size and number of associated periventricular hyperintensities on T2/FLAIR in the periatrial regions. Neuroimaging studies were also reviewed for cortical injuries as defined by abnormal signal intensity within any areas of the cortex with associated volume loss. The thalamic region was also evaluated for infarcts and tissue loss. The controls were children born at term (37–42 gestational weeks) with normal findings on conventional MR imaging performed in the same age range in childhood as the preterm cohort. The main clinical indications for performing imaging in the control group included headache, meningitis, and seizure activity. Clinical information was recorded on retrospective chart review for each patient and control. Seizure activity was further characterized by electroencephalography reports and classified as a 1-time occurrence (mostly febrile) or epilepsy (chronic repetitive seizures). The institutional review board at our medical center approved the study protocol.

MR Imaging Protocol

All imaging was performed in a 1.5T scanner (Signa LX; GE Healthcare, Milwaukee, Wisconsin) with a pediatric head coil. We acquired the following imaging sequences: axial fast spin-echo T2-weighted imaging (TE/TR = 85/5000 ms, FOV = 20 cm, matrix = 320 × 160 or 256 × 128, section thickness = 4–5 mm with 0- to 1-mm intersection gap); axial FLAIR imaging (TE/TR = 120/9000 ms, FOV = 20 cm, matrix = 320 × 160 or 256 × 128); and DTI protocol, which included an echo-planar imaging sequence (TE/TR = 80/10,000 ms, FOV = 22 cm, matrix = 128 × 128, section thickness = 5 mm, spacing = 0) applied along 25 noncollinear directions with a b-value of 1000 s/mm^2. For the volumetric analysis, the bilateral regions of the thalamus, seen on multiple axial sections, were manually traced on the T2-weighted sequence. The volume of the thalamus was computed from an area determined for all sections, section thicknesses, and gaps between the sections.

DTI Postprocessing

All DTI data were extracted by using DTIStudio (Johns Hopkins University, Baltimore, Maryland). The anterior, lateral, medial, and posterior subdivisions of the thalamus were determined by reference to the *Stereotactic Atlas of the Human Thalamus and Basal Ganglia* by Anne Morel.[24-26] Small circular regions of interest with a diameter of 4 mm were positioned in the anterior, lateral, medial, and posterior thalamus (Fig 1*A*). We followed Erbetta et al[24] for specifics about placing these regions of interest for the nuclei. The anterior region of interest was placed around the anterior nucleus in proximity to the genu of the internal capsule and posterolateral to the anterior columns of the fornix. The regions of interest for the medial and lateral subdivisions were placed at the level of the posterior limb of the internal capsule. The medial region of interest was placed near the third ventricle, and the lateral region of interest, close to the posterior limb of the internal capsule. The posterior region of interest was placed around the pulvinar nucleus. Analysis was performed on larger regions of interest, which together encompassed the entire thalamus (Fig 1*B*). The manual placement of the regions of interest was performed by the same person and checked by the same board-certified neuroradiologist to ensure consistency. The FA, RA, VR, λ_1, λ_2, λ_3, and ADC (or D_{av}) were recorded. λ_1 was also considered as $\lambda_\parallel$. $\lambda_\perp$ was calculated as the average of eigenvalues 2 and 3. See equations below:

$$1)\quad FA = \sqrt{\frac{3}{2}}\sqrt{\frac{(\lambda_1 - D_{av})^2 + (\lambda_2 - D_{av})^2 + (\lambda_3 - D_{av})^2}{\lambda_1^2 + \lambda_2^2 + \lambda_3^2}},$$

$$2)\quad RA = \frac{\sqrt{(\lambda_1 - D_{av})^2 + (\lambda_2 - D_{av})^2 + (\lambda_3 - D_{av})^2}}{\sqrt{3}D_{av}},$$

$$3)\quad VR = \frac{\lambda_1 \times \lambda_2 \times \lambda_3}{D_{av}^3},$$

$$4)\quad \lambda_\parallel = \lambda_1,$$

$$5)\quad \lambda_\perp = \left(\frac{\lambda_2 + \lambda_3}{2}\right),$$

$$6)\quad D_{av} = \left(\frac{\lambda_1 + \lambda_2 + \lambda_3}{3}\right).$$

Statistical Analysis

ANOVA was used to compare the DTI metrics and volume of the thalamus and its subdivisions between the PVL and control groups. Pearson correlations were calculated to measure the association be-

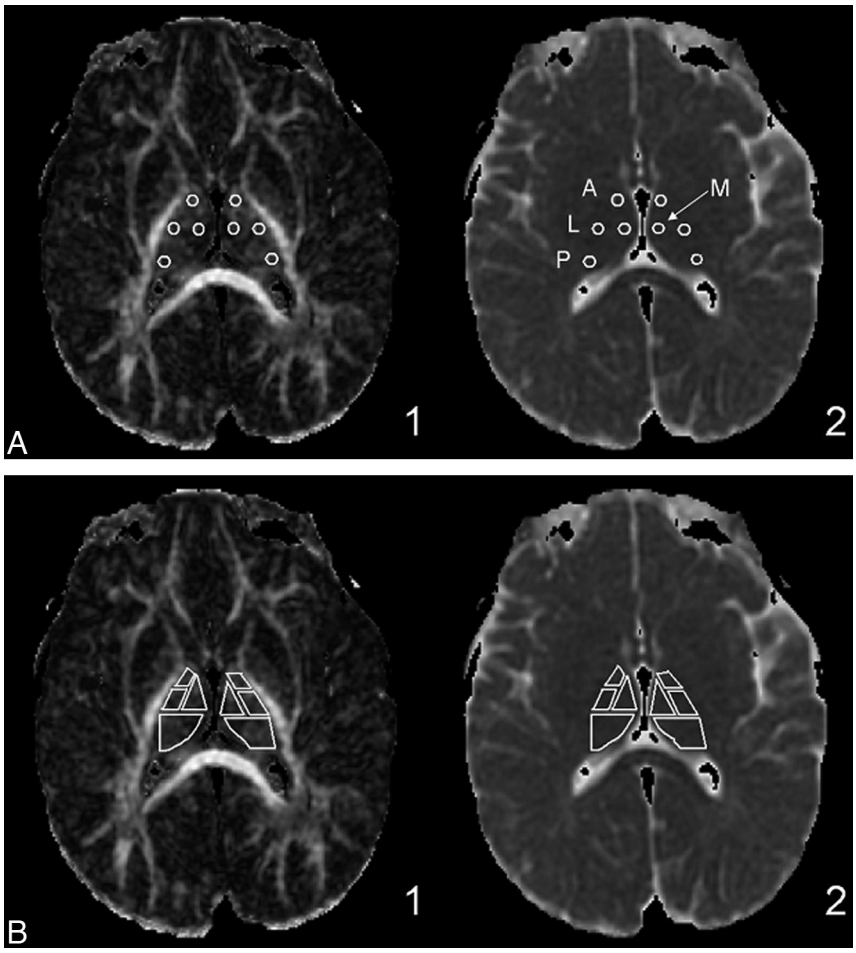

Fig 1. Thalamic subdivision small and large region-of-interest anatomic locations. *A,* The small circular regions of interest are fixed at a diameter of 4 mm. Region-of-interest placements in the anterior, lateral, medial, and posterior (pulvinar) nuclei of the thalamus are shown on the FA (1) and ADC (2) maps. *B,* Large region-of-interest subdivisions are shown on the same FA and ADC maps.

tween pairs of variables. The amount of variation explained by a linear regression was estimated by R^2. A Student *t* test was used to compare the ages between groups. Differences between patients with PVL and controls for sex, seizure activity, and other categoric clinical variables were compared by using the test of 2 binomial proportions. The Fisher exact test was used for differences on ethnicity, sex, cerebral palsy, and cortical injury. The Fisher exact test was used when the χ^2 test could not be performed due to a small sample size. Minitab Statistical Software (Minitab, State College, Pennsylvania) was used for statistical analyses.

Results

Clinical Data Base

The volumetric study included 17 patients with PVL (mean PCA, 5.6 ± 4 years; range, 1.0–14.3 years) and 74 controls (mean PCA, 5.9 ± 3.4 years; range, 1.8–12.7 years). The patients with PVL were born at 24–36 gestational weeks and were similar in PCA to the control group ($P = .90$). Of these subjects, a subset of 16 patients with PVL (mean PCA, 5.7 ± 4.1 years; range, 1.0–14.3 years) and 68 controls (mean PCA, 6.0 ± 3.4 years; range, 1.8–12.7 years) underwent DTI assessments due to the necessity of excluding DTI data in certain children with artifactual movement during imaging. Among the patients with PVL with available neurologic information, 100% demonstrated developmental delay, and 81%, cerebral palsy, the latter all subclassified as spastic—all significant differences from the controls ($P < .001$). Most (67%) of the patients with PVL also had a history of seizures, primarily classified as epilepsy, in comparison with 26% of the controls, the latter mainly classified as having febrile seizures ($P = .003$). There was no statistically significant difference between patients with PVL and controls with respect to race or sex.

Conventional MR Imaging Findings of the Cerebral White Matter

As per study inclusion criteria, all of the patients with PVL had cerebral white matter damage on conventional MR imaging, whereas the controls did not. The T2/FLAIR signal-intensity hyperintensities in the patients with PVL were both focal and confluent and were found in the parieto-occipital white matter and the region of the optic radiations in 100% of the cases. The severity of white matter injury was observed in T2, FLAIR, FA, and ADC images (Fig 2). None of the patients with PVL demonstrated focal T2/FLAIR hyperintensities in the deep frontal white matter, and 12% of the patients with PVL had cortical injury (Table 1).

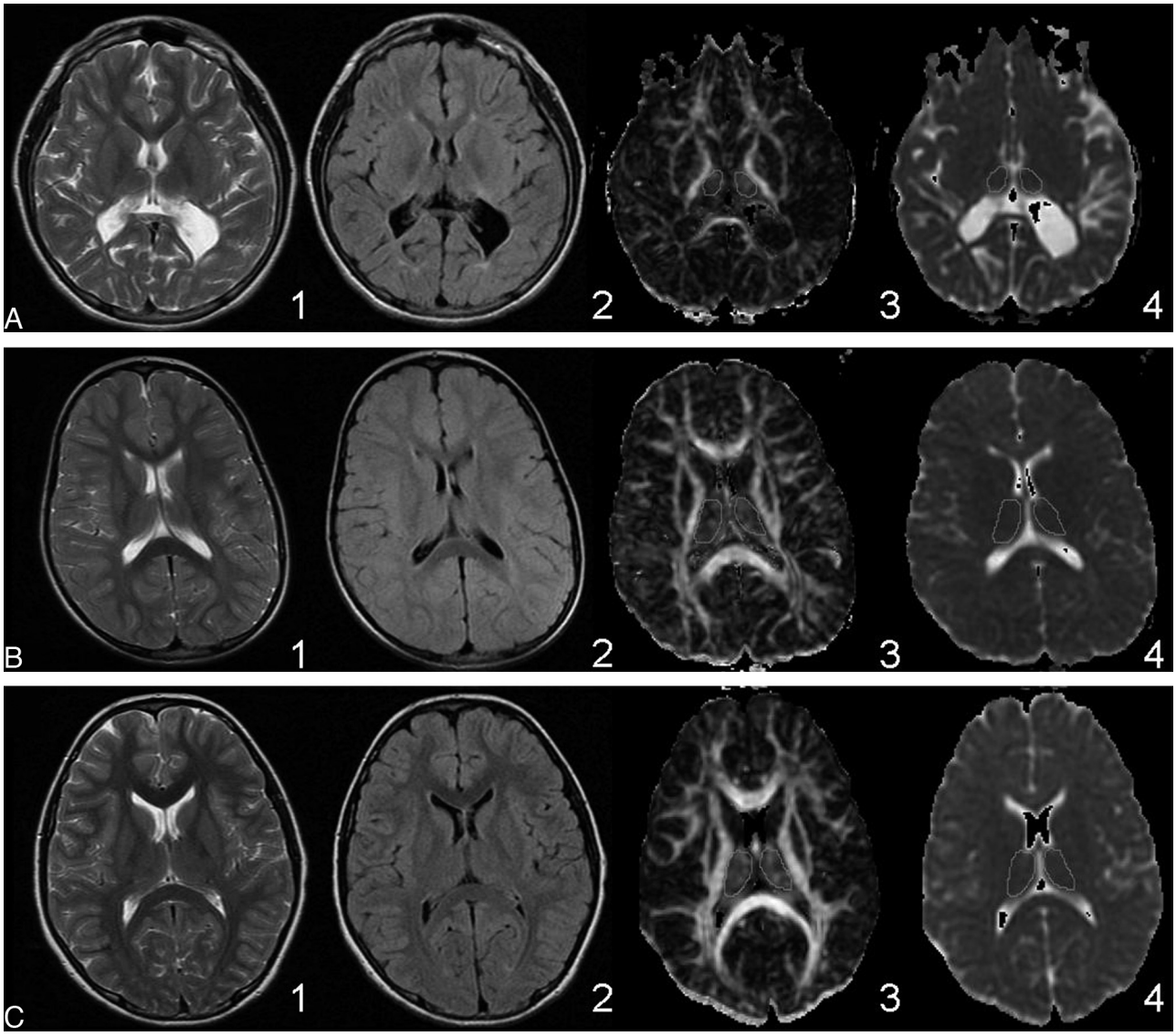

Fig 2. Range of severity of PVL and whole thalamic regions of interest. Rows: *A*, Severe PVL. *B*, Mild PVL. *C*, Healthy control. Columns: 1) T2-weighted. 2) FLAIR. 3) FA. 4) ADC. The T2 and FLAIR images for the patients with PVL show periventricular hyperintensity. The severity of PVL in each case is evident from the degree of periventricular white matter volume loss compared with the control. The contours for acquiring the DTI metrics are shown on the FA and ADC images for the whole thalamus.

Table 1: Volumetric analysis of the entire thalamus

	Mean (SD)		
	PVL (n = 17)	Control (n = 74)	P Value
PCA (yr)	5.6 (4.0)	5.9 (3.4)	.779[a]
Thalamic volume (mm^3)	5588 (2081)	9750 (1501)	<.0001[a]
Cortical injury	12% (2)	0% (0)	.00[b]

[a] ANOVA.
[b] Fisher exact test.

Overall Volume Measurements of the Thalamus

With MR imaging, the volume of the thalamus in patients with PVL (5588 ± 2081 mm^3) was significantly smaller than that in controls (9750 ± 1501 mm^3) ($P < .0001$) (Table 1). Patients with severe PVL ($n = 4$) demonstrated a marked decrease in thalamic volume (3360 ± 1155 mm^3) compared the thalamic volumes of patients with moderate PVL ($n = 9$) (6089 ± 1728 mm^3) or mild PVL (6687 ± 2194 mm^3) ($n = 4$) ($P = .032$). There was no significant correlation between thalamic volume and PCA in the age range studied (1.0–14.3 years) in either the PVL or the control group.

Diffusion Tensor Metrics of the Entire Thalamus

The paired mean differences between the left and right regions of the thalamus and its subdivisions were not significantly different from zero for all DTI measurements (paired t tests); hence, the values from the bilateral regions were averaged for subsequent analyses. The preterm group with PVL had significantly decreased FA ($P = .003$), RA ($P = .004$), and VR ($P = .008$) in the entire thalamus compared with the control group (Table 2). There was no statistically significant age effect on the anisotropy metrics (data not shown). The $\lambda_\perp$ was increased ($P = .02$) in preterm infants with PVL compared with controls. The $\lambda_\parallel$, however, was similar between the 2 groups (Table 2). There was a nonsignificant trend toward increased mean diffusivity in patients with PVL compared with the controls ($P = .056$).

Table 2: DTI analysis of the entire thalamus

	Mean (SD)		
	PVL[a] (n = 16)	Control[a] (n = 68)	P Value[b]
PCA (yr)	5.7 (4.1)	6.0 (3.4)	.80
FA	0.24 (0.02)	0.26 (0.02)	.003
RA	0.20 (0.02)	0.22 (0.02)	.004
VR	0.07 (0.01)	0.08 (0.01)	.008
$\lambda_{\parallel}$ ($\times 10^{-3}$ mm^2/s)	1.04 (0.13)	1.01 (0.07)	.215
$\lambda_{\perp}$ ($\times 10^{-3}$ mm^2/s)	0.73 (0.10)	0.69 (0.05)	.020
ADC ($\times 10^{-3}$ mm^2/s)	0.83 (0.11)	0.79 (0.06)	.056

[a] DTI data excluded in certain children with artifactual movement during imaging.
[b] ANOVA.

Table 3: DTI analyses of thalamic subdivisions

	Mean (±SD)		
	PVL (n = 16)	Control (n = 68)	P Value[a]
Anterior thalamus			
FA	0.30 (0.04)	0.30 (0.04)	.828
RA	0.25 (0.03)	0.25 (0.04)	.802
$\lambda_{\parallel}$ ($\times 10^{-3}$ mm^2/s)	1.00 (0.08)	1.02 (0.07)	.335
$\lambda_{\perp}$ ($\times 10^{-3}$ mm^2/s)	0.65 (0.06)	0.66 (0.05)	.519
ADC ($\times 10^{-3}$ mm^2/s)	0.77 (0.06)	0.78 (0.05)	.348
Medial thalamus			
FA	0.23 (0.03)	0.25 (0.04)	.116
RA	0.20 (0.03)	0.21 (0.03)	.113
$\lambda_{\parallel}$ ($\times 10^{-3}$ mm^2/s)	0.95 (0.09)	0.96 (0.07)	.430
$\lambda_{\perp}$ ($\times 10^{-3}$ mm^2/s)	0.68 (0.07)	0.69 (0.05)	.881
ADC ($\times 10^{-3}$ mm^2/s)	0.77 (0.08)	0.78 (0.05)	.584
Lateral thalamus			
FA	0.29 (0.06)	0.28 (0.05)	.650
RA	0.25 (0.05)	0.24 (0.05)	.649
$\lambda_{\parallel}$ ($\times 10^{-3}$ mm^2/s)	1.00 (0.11)	0.98 (0.09)	.371
$\lambda_{\perp}$ ($\times 10^{-3}$ mm^2/s)	0.64 (0.07)	0.64 (0.05)	.834
ADC ($\times 10^{-3}$ mm^2/s)	0.76 (0.07)	0.75 (0.05)	.734
Pulvinar thalamus			
FA	0.25 (0.03)	0.24 (0.03)	.794
RA	0.21 (0.03)	0.20 (0.02)	.882
$\lambda_{\parallel}$ ($\times 10^{-3}$ mm^2/s)	1.04 (0.11)	0.98 (0.07)	.007
$\lambda_{\perp}$ ($\times 10^{-3}$ mm^2/s)	0.72 (0.08)	0.68 (0.05)	.024
ADC ($\times 10^{-3}$ mm^2/s)	0.83 (0.09)	0.78 (0.06)	.011

[a] ANOVA.

Diffusion Tensor Metrics of the Subdivisions of the Thalamus

All 3 diffusivity measurements in the pulvinar were significantly increased in the patients with PVL compared with controls: $\lambda_{\parallel}$ ($P = .007$), $\lambda_{\perp}$ ($P = .024$), and D_{av} ($P = .011$) (Table 3). There was no difference between the PVL and control groups in these metrics in the anterior, medial, and lateral subdivisions. There was also no difference in the FA and RA metrics between the patients with PVL and controls in any thalamic subdivision, including the pulvinar. The same findings were essentially reproduced between the large and small subdivision regions of interest with selective diffusivity abnormality within the pulvinar again noted.

Correlation between DTI Metrics and Severity of White Matter Injury in the Pulvinar

We asked whether the DTI metrics positively correlated with the degree of PVL (ie, were the DTI metrics worse in moderate or severe PVL compared with mild PVL?). Although the sample size was small in the mild, moderate, and severe PVL groups (Table 4), we found that the $\lambda_{\perp}$ values of the whole thalamus and pulvinar were significantly increased in the moderate/severe groups compared with the mild groups (whole thalamus, $P = .013$; pulvinar, $P = .024$) and that the $\lambda_{\parallel}$ in the pulvinar in mild PVL was significantly decreased compared with severe PVL ($P = .026$).

Discussion

This study reports bilateral thalamic atrophy with microstructural abnormalities preferentially involving the pulvinar in childhood survivors of prematurity with PVL and neurologic disabilities. The major findings of this study are the following: 1) a high incidence of developmental disabilities and cerebral palsy in the PVL group; 2) a significant reduction in the overall volume of the thalamus in patients with PVL compared with controls; 3) a significant association of severe PVL, as assessed by quantitative measures, with the most severe decrease in overall thalamic volume; 4) preferential damage to the pulvinar in PVL relative to the anterior, medial, and lateral subdivisions; 5) significantly decreased FA and increased $\lambda_{\perp}$ in the thalamic parenchyma overall and increased axial, radial, and mean diffusivities in the pulvinar parenchyma, suggesting injury to afferent and efferent myelinated axons; and 6) a positive correlation of pulvinar abnormalities with those of the posterior (parieto-occipital) white matter in PVL, suggesting that the pathologic changes in the pulvinar reflect, as least in part, secondary effects of the injury to interconnections between the pulvinar and parieto-occipital cortices in the cognitive visual network. Together, our findings indicate that bilateral and widespread thalamic volume loss and abnormal DTI metrics correlate with global neurodevelopmental disabilities in long-term survivors with PVL and suggest that selective microstructural damage in the pulvinar likely contributes to abnormal cognitive visual processing, which is known to occur in such survivors. Decreased thalamic volume has been reported previously in preterm survivors,[11-13,27-29] including those with PVL.[11-13] Our study is unique in its analysis of combined volumetric and microstructural (DTI) measurements that point to the simultaneous occurrence of different types of thalamic lesions (ie, thalamic atrophy due to neuronal loss and gliosis combined with myelinated axonal injury).

Microstructural Abnormalities in the Thalamus in PVL

In the study cohort of patients with PVL compared with controls using DTI, we found decreased FA and increased $\lambda_{\perp}$ throughout the entire thalamic parenchyma and increased axial, radial, and mean diffusivities throughout the pulvinar. Although the pathologic significance of DTI metrics is somewhat controversial, abnormalities of $\lambda_{\parallel}$ are generally considered to indicate axonal pathology, while increased $\lambda_{\perp}$ is thought to be related to primary demyelination.[30-34] In the acute phase of axonal damage, $\lambda_{\parallel}$ is decreased on the basis of correlations between neuroimaging and quantitative staining for neurofilaments in tissue sections in animal models.[32] With time, however, $\lambda_{\parallel}$ may increase due to an increase in the extra-axonal space, which reflects reduced axonal attenuation or axonal caliber.[35-37] Because damage in the patients with PVL of our cohort was preferentially in the parieto-occipital white matter that contains axons to and from the pulvinar (see be-

Table 4: Correlation of DTI metrics and severity of white matter injury

	Mean (±SD)				*P* Value	
	1	2	3	4		
	Control ($n = 68$)	Mild ($n = 4$)	Moderate ($n = 8$)	Severe ($n = 4$)	1 vs 2 vs 3 vs 4	2 vs 3 vs 4
Entire thalamus						
FA	0.26 (0.02)	0.25 (0.030	0.23 (0.01)	0.26 (0.01)	.003	.069
$\lambda_{\perp}$ ($\times 10^{-3}$ mm^2/s)	0.69 (0.05)	0.63 (0.06)	0.79 (0.08)	0.71 (0.08)	.000	.013
Pulvinar						
$\lambda_{\parallel}$ ($\times 10^{-3}$ mm^2/s)	0.98 (0.07)	0.91 (0.15)	1.08 (0.07)	1.08 (0.07)	.000	.026
$\lambda_{\perp}$ ($\times 10^{-3}$ mm^2/s)	0.68 (0.05)	0.63 (0.07)	0.76 (0.06)	0.71 (0.06)	.000	.024

low), the abnormal DTI metrics in this structure likely reflect degeneration of these axons and secondary myelin changes (wallerian degeneration). This possibility is supported by the finding of axonal damage, as determined with an antibody to fractin, a marker of axonal injury, within the thalamic parenchyma in 59% of the patients with PVL at postmortem examination.[4] In addition, diffuse and widespread axonal damage has been found in the gliotic white matter surrounding periventricular necrotic foci.[38] The loss of overall thalamic volume in patients with PVL in our cohort represents, as opposed to abnormal DTI metrics, primary and/or trans-synaptic neuronal loss and gliosis, based on extrapolations from pathologic studies of the thalamus in PVL.[4,14]

Clinical Consequences of Thalamic Damage in PVL

The findings of volume loss and decreased anisotropy in the thalamus of childhood survivors with PVL and developmental disabilities, seizures, and/or cerebral palsy in our cohort suggest that thalamic damage in combination with PVL results in significant and diverse neurologic dysfunction. Indeed, symmetric and bilateral thalamic loss in isolation is known to contribute to global cognitive, limbic, sensory, motor, and state deficits,[39] given the role of the thalamus in each of these functions via extensive reciprocal interconnections to related areas in the cerebral cortex.[40] Yet, the major brunt of the thalamic damage in our cohort occurred to the pulvinar, begging the question of the function of this structure. The pulvinar is a critical component of the parietal cortical-subcortical network that mediates visual attention and visuospatial integration, the so-called posterior visual attention network.[41-46]

Premature infants with PVL who survive into childhood demonstrate so-called CVI, which reflects an impaired capacity to process visual information and occurs with little or no compromise in visual acuity[46]; deficits occur in visual object recognition, visual-spatial skills, and visual memory.[46] The anatomic basis of CVI in preterm infants with PVL is thought to be the destruction of the interconnections of the posterior visual network by preferential damage to the parieto-occipital white matter and distal optic radiations relative to the frontal white matter.[14,46–52] Moreover, DTI with tractography demonstrates frequent injury to the posterior thalamic radiation, among other tracts, which connects the pulvinar and lateral geniculate nucleus to the parietal cortex.[53,54] Of major interest to our study is the report of clinical dysfunction in attention-demanding visual integration in adolescents with PVL, who demonstrate preferential white matter damage to periventricular parieto-occipital regions, presumably destroying the thalamocortical interconnections of the posterior visual attention network.[55] Lesions of the pulvinar detected by conventional MR imaging in childhood survivors of prematurity with PVL have also been correlated with paroxysmal ocular downward deviation, as well as global developmental disabilities.[6] Correlations in visual-spatial function with pulvinar damage are not possible in our study because the relevant neuropsychological testing could not be performed. Nevertheless, our study suggests that CVI in preterm survivors with PVL can involve (primary and/or secondary) damage to the pulvinar in combination with damage to the posterior white matter in the parieto-occipital regions, optic radiation, and/or posterior thalamic radiation.

Limitations of the Study

A limitation of the study is its retrospective nature with the determination of the neurologic disabilities of patients based on chart review. Thus, it was not possible to make precise correlations between the spectrum of neurologic abnormalities, including sophisticated cognitive visual or other testing, to uncover subtle deficits potentially related to the pulvinar or other thalamic subnuclei. Another limitation of the study is the analysis of children with neurologic indications for MR imaging as controls who may not be healthy and thus may not truly represent a healthy population. Nevertheless, the neurologic indications for neuroimaging in the controls were considered minor and typically resolved (eg, meningitis, febrile seizures, or unconfirmed developmental delay).

Conclusions

We report major thalamic abnormalities in childhood survivors of prematurity with PVL. In addition, we report novel microstructural abnormalities in the entire thalamus and pulvinar that likely reflect damage to thalamic axons at their sites of origin or targets. The damage to the pulvinar correlates with pathology in the parieto-occipital white matter, suggesting that the damage to the pulvinar reflects preferential injury to the posterior white matter with severance of parieto-occipital connections to and from it. Finally, our study indicates a broad spectrum of injury to the thalamus in childhood survivors of prematurity and perinatal white matter injury.

Acknowledgments

We thank Julia Castro for help with manuscript preparation and Drs Hanna Damásio, Mathew Borzage, and Jessica Wisnowski for helpful comments with the manuscript.

References

1. Volpe JJ. **Brain injury in premature infants: a complex amalgam of destructive and developmental disturbances.** *Lancet Neurol* 2009;8:110–24
2. Kinney HC, Volpe JJ. **Perinatal panencephalopathy in premature infants: is it due to hypoxia-ischemia? Brain hypoxia and ischemia.** In: Haddad GG, Yu SP, eds. *Brain Hypoxia and Ischemia with Special Emphasis on Development.* New York: Humana Press; 2009:153–86
3. Leviton A, Gilles FH. **Acquired perinatal leukoencephalopathy.** *Ann Neurol* 1984;16:1–8
4. Ligam P, Haynes R, Folkerth RD, et al. **Thalamic damage in periventricular leukomalacia: novel pathologic observations relevant to cognitive deficits in survivors of prematurity.** *Pediatr Res* 2009;65:524–29
5. Ricci D, Anker S, Cowan F, et al. **Thalamic atrophy in infants with PVL and cerebral visual impairment.** *Early Hum Dev* 2006;82:591–95
6. Yokochi K. **Thalamic lesions revealed by MR associated with periventricular leukomalacia and clinical profiles of subjects.** *Acta Paediatr* 1997;86:493–96
7. Giménez M, Junqué C, Narberhaus A, et al. **Correlations of thalamic reductions with verbal fluency impairment in those born prematurely.** *Neuroreport* 2006;17:463–66
8. Boardman JP, Counsell SJ, Rueckert D, et al. **Abnormal deep grey matter development following preterm birth detected using deformation-based morphometry.** *Neuroimage* 2006;32:70–78
9. Lin Y, Okumura A, Hayakawa F, et al. **Quantitative evaluation of thalami and basal ganglia in infants with periventricular leukomalacia.** *Dev Med Child Neurol* 2001;43:481–85
10. Nosarti C, Giouroukou E, Healy E, et al. **Grey and white matter distribution in very preterm adolescents mediates neurodevelopmental outcome.** *Brain* 2008; 131(pt 1):205–17. Epub 2007 Dec 3
11. Inder TE, Warfield SK, Wang H, et al. **Abnormal cerebral structure is present at term in premature infants.** *Pediatrics* 2005;115:286–94
12. Woodward LJ, Anderson PJ, Austin NC, et al. **Neonatal MRI to predict neurodevelopmental outcomes in preterm infants.** *N Engl J Med* 2006;355:685–94
13. Thompson DK, Warfield SK, Carlin JB, et al. **Perinatal risk factors altering regional brain structure in the preterm infant.** *Brain* 2007;130:667–77
14. Pierson CR, Folkerth RD, Billiards SS, et al. **Gray matter injury associated with periventricular leukomalacia in the premature infant.** *Acta Neuropathol* 2007;114:619–31
15. Basser PJ. **Inferring microstructural features and the physiological state of tissues from diffusion-weighted images.** *NMR Biomed* 1995;8:333–44
16. Beaulieu C. **The basis of anisotropic water diffusion in the nervous system: a technical review.** *NMR Biomed* 2002;15:435–55
17. Song S, Sun S, Ramsbottom MJ, et al. **Dysmyelination revealed through MRI as increased radial (but unchanged axial) diffusion of water.** *Neuroimage* 2002;17:1429–36
18. Song S, Sun S, Ju W, et al. **Diffusion tensor imaging detects and differentiates axon and myelin degeneration in mouse optic nerve after retinal ischemia.** *Neuroimage* 2003;20:1714–22
19. Sun SW, Kuabm HF, Le TQ, et al. **Differential sensitivity of in vivo and ex vivo diffusion tensor imaging to evolving optic nerve injury in mice with retinal ischemia.** *Neuroimage* 2006;32:1195–204
20. Counsell SJ, Dyet LE, Larkman DJ, et al. **Thalamo-cortical connectivity in children born preterm mapped using probabilistic magnetic resonance tractography.** *Neuroimage* 2007;34:896–904
21. Hoon AH, Stashinko EE, Nagae LM, et al. **Sensory and motor deficits in children with cerebral palsy born preterm correlate with diffusion tensor imaging abnormalities in thalamocortical pathways.** *Dev Med Child Neurol* 2009; 51:697–704
22. Nagae LM, Hoon AH, Stashinkon K, et al. **Diffusion tensor imaging in children with periventricular leukomalacia: variability of injuries to white matter tracts.** *AJNR Am J Neuroradiol* 2007;28:1213–22
23. Panigrahy A, Barnes PD, Robertson RL, et al. **Volumetric brain differences in children with periventricular T2 signal hyperintensities: a grouping by gestational age at birth.** *AJR Am J Roentgenol* 2001;177:695–702
24. Erbetta A, Mandelli M, Savoiardo M, et al. **Diffusion tensor imaging shows different topographic involvement of the thalamus in progressive supranuclear palsy and corticobasal degeneration.** *AJNR Am J Neuroradiol* 2009; 30:1482–87
25. Niemann K, Mennicken VR, Jeanmonod D, et al. **The Morel Stereotactic Atlas of the Human Thalamus: atlas-to-MR registration of internally consistent canonical model.** *Neuroimage* 2000;12:601–16
26. Wiegell MR, Tuch DS, Larsson HB, et al. **Automatic segmentation of thalamic nuclei from diffusion tensor magnetic resonance imaging.** *Neuroimage* 2003;19:391–401
27. Peterson BS, Vohr B, Staib LH, et al. **Regional brain volume abnormalities and long-term cognitive outcome in preterm infants.** *JAMA* 2000;284:1939–47
28. Nosarti C, Al-Asady MH, Frangou S, et al. **Adolescents who were born very preterm have decreased brain volumes.** *Brain* 2002;125:1616–23
29. Kesler SR, Ment LR, Vohr B, et al. **Volumetric analysis of regional cerebral development in preterm children.** *Pediatr Neurol* 2004;31:318–25
30. Song S, Yoshino J, Le TQ, et al. **Demyelination increases radial diffusivity in corpus callosum of mouse brain.** *Neuroimage* 2005;26:132–40
31. Zhang J, Jones M, DeBoy CA, et al. **Diffusion tensor magnetic resonance imaging of wallerian degeneration in rat spinal cord after dorsal root axotomy.** *J Neurosci* 2009;29:3160–71
32. Buddle MD, Xie M, Cross AH, et al. **Axial diffusivity is the primary correlate of axonal injury in the experimental autoimmune encephalomyelitis spinal cord: a quantitative pixelwise analysis.** *J Neuosci* 2009;29:2805–13
33. Naismith RT, Xu J, Tutlam NT, et al. **Disability in optic neuritis correlates with diffusion tensor-derived directional diffusivities.** *Neurology* 2009;72:589–94
34. Kumar R, Macey PM, Woo MA, et al. **Diffusion tensor imaging demonstrates brainstem and cerebellar abnormalities in congenital central hypoventilation syndrome.** *Pediatr Res* 2008;64:275–80
35. Ludeman NA, Berman JI, Wu YW, et al. **Diffusion tensor imaging of the pyramidal tracts in infants with motor dysfunction.** *Neurology* 2008;71:1676–82
36. Agosta F, Benedetti B, Rocca MA, et al. **Quantification of cervical cord pathology in primary progressive MS using diffusion tensor MRI.** *Neurology* 2005; 64:631–35
37. Cheong J, Thompson D, Wang H, et al. **Abnormal white matter signal on MR imaging is related to abnormal tissue microstructure.** *AJNR Am J Neuroradiol* 2009;30:623–28
38. Haynes RL, Billiards SS, Borenstein NS, et al. **Diffuse axonal injury in periventricular leukomalacia as determined by apoptotic marker fractin.** *Pediatr Res* 2008;63:656–61
39. Kinney HC, Korein J, Panigrahy A, et al. **Neuropathological findings in the brain of Karen Ann Quinlan: the role of the thalamus in the persistent vegetative state.** *N Engl J Med* 1994;330:1469–75
40. Jones, E. *The Thalamus.* 2nd ed. Cambridge, UK: Cambridge University Press; 2006
41. Corbetta M, Shulman GL, Miezin FM, et al. **Superior parietal cortex activation during spatial attention shifts and visual feature conjunction.** *Science* 1995;270:802–05
42. Shafritz KM, Gore JC, Marois R. **The role of the parietal cortex in visual feature binding.** *Proc Natl Acad Sci U S A* 2002;99:10917–22
43. Friedman-Hill SR, Robertson LC, Desimone R, et al. **Posterior parietal cortex and the filtering of distractors.** *Proc Natl Acad Sci U S A* 2003;100:4263–68. Epub 2003 Mar 19
44. Ward R, Danziger S, Owen V, et al. **Deficits in spatial coding and feature binding following damage to spatiotopic maps in the human pulvinar.** *Nat Neurosci* 2002;5:99–100
45. Kastner S, O'Connor DH, Fukui MM, et al. **Functional imaging of the human lateral geniculate nucleus and pulvinar.** *J Neurophysiol* 2004;91:438–48
46. Fazzi E, Bova S, Giovenzana A, et al. **Cognitive visual dysfunctions in preterm children with periventricular leukomalacia.** *Dev Med Child Neurol* 2009; 51:974–81
47. Banker BQ, Larroche JC. **Periventricular leukomalacia of infancy: a form of neonatal anoxic encephalopathy.** *Arch Neurol* 1962;7:386–410
48. Uggetti C, Egitto M, Fazzi E, et al. **Cerebral visual impairment in periventricular leukomalacia: MR correlation.** *AJNR Am J Neuroradiol* 1996;17:979–85
49. Hoyt CS. **Visual function in the brain-damaged child.** *Eye* 2003;17:369–84
50. Jacobson LK, Dutton GN. **Periventricular leukomalacia: an important cause of visual and ocular motility dysfunction in children.** *Surv Ophthalmol* 2000;45:1–13
51. Cioni G, Bertuccelli B, Boldrini A, et al. **Correlation between visual function, neurodevelopmental outcome, and magnetic resonance imaging findings in infants with periventricular leucomalacia.** *Arch Dis Child Fetal Neonatal Ed* 2000;82:F134–40
52. Jacobson L, Lundin S, Flodmark O, et al. **Periventricular leukomalacia causes visual impairment in preterm children: a study on the aetiologies of visual impairment in a population-based group of preterm children born 1989–95 in the county of Värmland, Sweden.** *Acta Ophthalmol Scand* 1998;76:593–98
53. Hoon AH, Lawrie WT, Melhem ER, et al. **Diffusion tensor imaging of periventricular leukomalacia shows affected sensory cortex white matter pathways.** *Neurology* 2002;59:752–56
54. Behrens TE, Johansen-Berg H, Woolrich MW, et al. **Non-invasive mapping of connections between human thalamus and cortex using diffusion imaging.** *Nat Neurosci* 2003;6:750–57
55. Pavolova M, Sokolov A, Staudt M, et al. **Recruitment of periventricular parietal regions in processing cluttered point-light biological motion.** *Cereb Cortex* 2004;5:594–601